Supplement

Supplemental Acknowledgements

The Competence Network for Congenital Heart Defects and the National Register for Congenital Heart Defects are funded by the German Center for Cardiovascular Research (DZHK). Sample collection sites were Universitätsklinikum Schleswig-Holstein/Kiel (Hans-Heiner Kramer), Deutsches Herzzentrum Berlin (Felix Berger), Universitätsklinikum Erlangen (Okan Toka), Universitäts-Herzzentrum Bad Krozingen/Freiburg (Brigitte Stiller), Herzzentrum Leipzig (Ingo Daehnert), and Universitätsklinikum Saarland/Homburg (Hashim Abdul-Khaliq).

Supplemental Movies and Figures

Movie S1: Mitochondria are spatially close to the basal body.

A tilt series of human fibroblasts was produced via tomo-cryo-electron microscopy. A 3D reconstruction was generated and different organelles labeled by segmentation. Mitochondria are labeled in blue, the mother centriole in pink, appendages of the mother centriole in yellow, and the daughter centriole in orange. Additionally, selected microtubules connected to the mother centriole are shown in purple, while a microtubule projecting from appendages of the mother centriole towards mitochondria is labeled green. The horizontal field width corresponds to 2.8 µm.

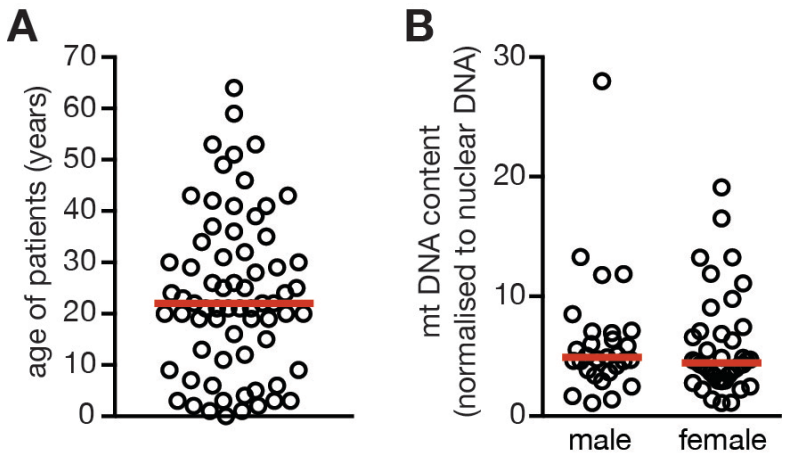

Figure S1: Characterization of heterotaxy patient cohort.

A, Age distribution of heterotaxy patients. Median age is indicated by line.

B, Gender does not influence mitochondrial DNA content in heterotaxy patients. Female n= 40, male n= 29. The bar represents the median.

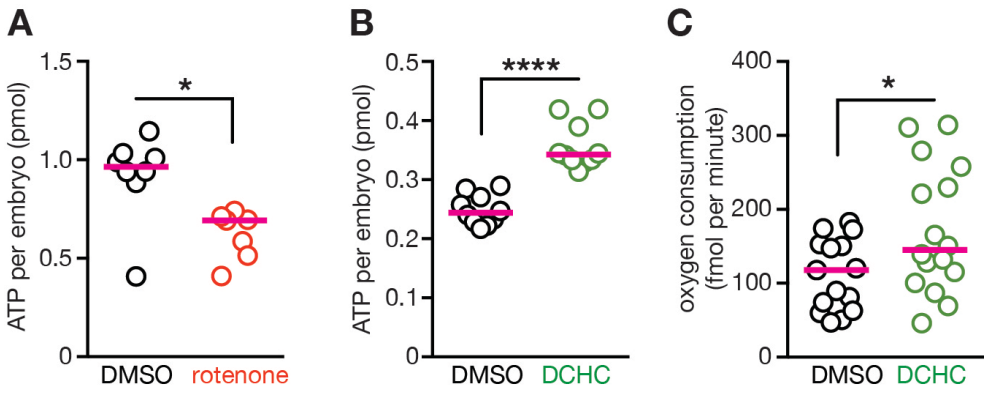

Figure S2: Manipulation of mitochondrial function in zebrafish embryos.

A, Rotenone treatment reduces ATP content in 8 ss zebrafish embryos as measured by luminescence-based ATP detection. Two-tailed Mann-Whitney test, N=1, n=8/7, p=0.014.

B, Treatment with 3-(2,4-dichlorophenyl)-7-hydroxy-4H-chromen-4-one (DCHC) elevates ATP content in 8 ss zebrafish embryos. Two-tailed Mann-Whitney test, N=1, n=10/10, $p<0.0001$.

C, Treatment with DCHC increases oxygen consumption in 8 ss zebrafish embryos. Two-tailed t-test with Welch's correction, N=1, n=15/16, p=0.0253.

The bar represents the median.

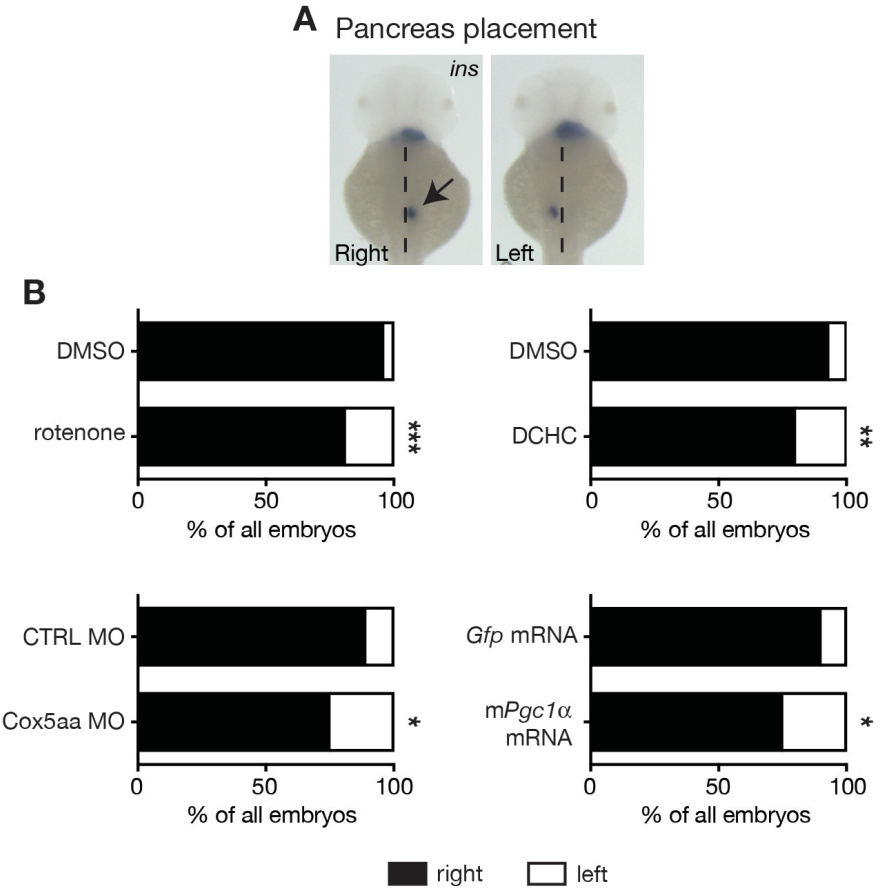

Figure S3: Altered mitochondrial function increased irregular placement of pancreas.

A, Pancreas placement was visualized by *in situ* hybridization for *ins*. Shown is correct placement of the pancreas right of the midline (indicated by arrow) as well as irregular placement on the left. The midline is indicated by a dashed line.

B, Quantitative assessment of pancreas placement. Two-sided Fisher's exact test; DMSO vs rotenone (rot), N=6, n=109/111, p=0.0005; DMSO vs DCHC, N=4, n=111/115, p=0.0063; CTRL MO vs Cox5aa MO, N=3, n=66/76, p=0.0308; *Gfp* mRNA vs m*Pgc1α* mRNA, N=3, n=72/79, p=0.0183.

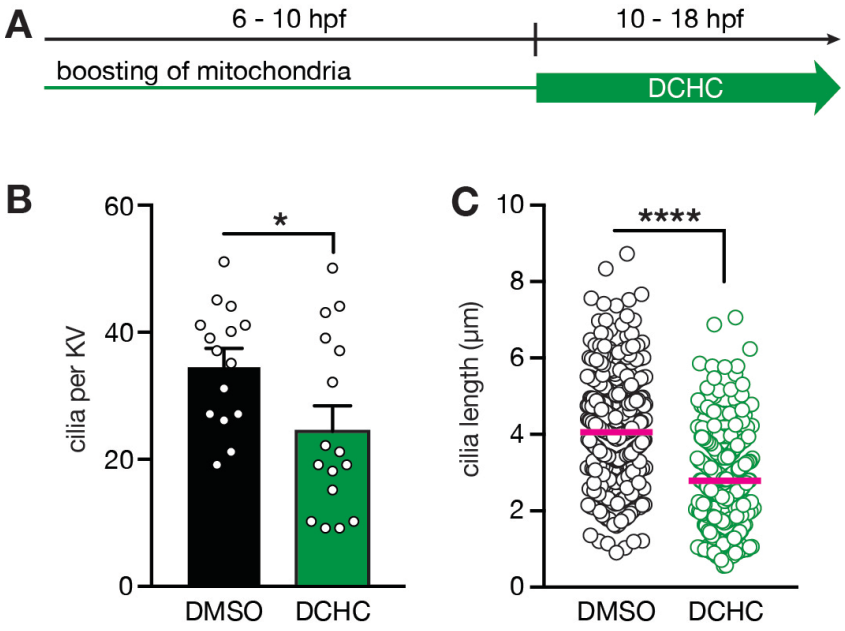

Figure S4: DCHC treatment of zebrafish embryos during stages in which ciliary function governs symmetry breaking reduces cilia number per KV and shortens nodal cilia similarly to treatment stages preceding KV formation.

A, Cilia were counted in KVs from zebrafish embryos treated with DMSO or DCHC, n=15/16, two-tailed student t test with Welch's correction, p=0.0244. Shown are mean ± SEM.

B, KV cilia are shortened in DCHC-treated embryos as compared to embryos treated with vehicle (DMSO); N=15/16, n=440/410, two-tailed Mann-Whitney test, p<0.0001. The bar represents the median.

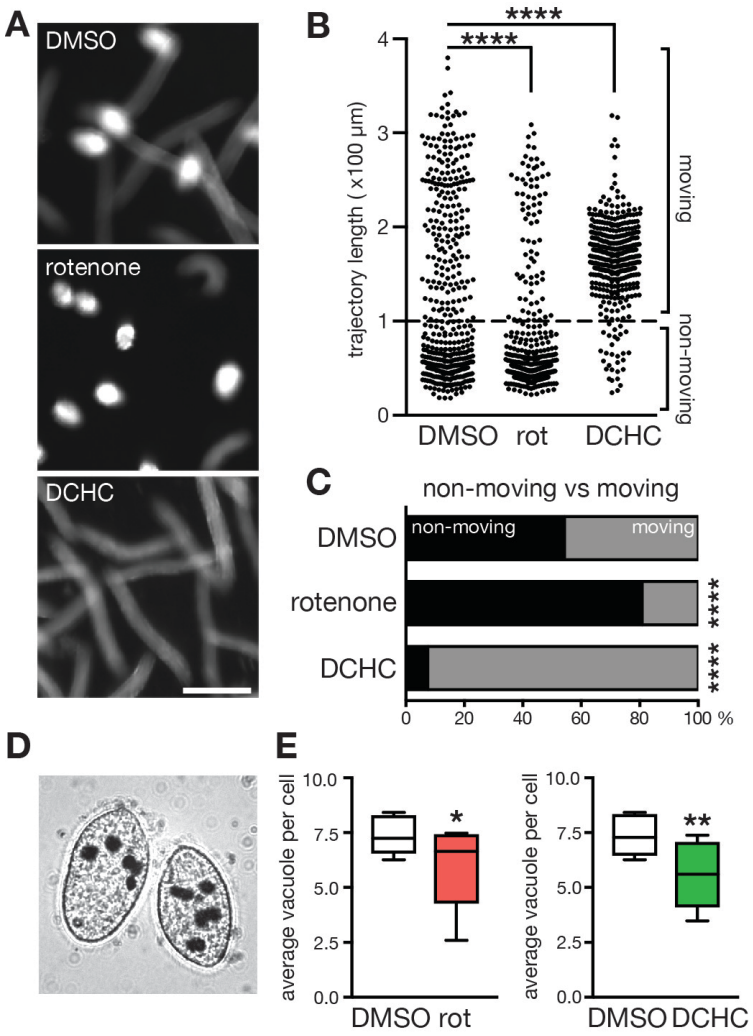

Figure S5: Cilia-dependent processes in *Tetrahymena thermophila* are sensitive to changes of mitochondrial function.

A, *Tetrahymena thermophila* depend on functional motile cilia for movement. Typical trajectories of swimming distance observed of *Tetrahymena* cells treated with DMSO, rotenone, or DCHC for 1 hour. Bright spots correspond to non-moving cells, while stripes reflect the distance of swimming cells. Pictures were taken with 10 s exposure. The scale bar: 100 µm.

B, Quantification of swimming distance. Kruskal-Wallis test with Dunn's correction, N=2, n=439/418/401, DMSO vs rotenone $p<0.0001$, DMSO vs DCHC $p<0.0001$.

C, Assessment of moving vs non-moving cells after mitochondrial manipulation. Two-tailed Fisher's exact test, N=2, n=440/418/401, DMSO vs rotenone $p<0.0001$, DMSO vs DCHC $p<0.0001$.

D, Motile cilia of the oral apparatus allow *Tetrahymena thermophila* to ingest food particles by phagocytosis. Shown are cells fed with drawing ink particles, which stain food vacuoles black.

E, Quantification of food vacuoles in *Tetrahymena thermophila* treated with DMSO, rotenone or DCHC during 1 hour. The average number of food vacuoles was calculated from each experiment and used for statistical analysis. Two-tailed, paired t-test; DMSO vs rotenone, N=6, n=730/707, p=0.044; DMSO vs DCHC, N=5, n=608/610, p=0.0034. Box and whiskers plot showing median, first and third quartile, minimum and maximum.

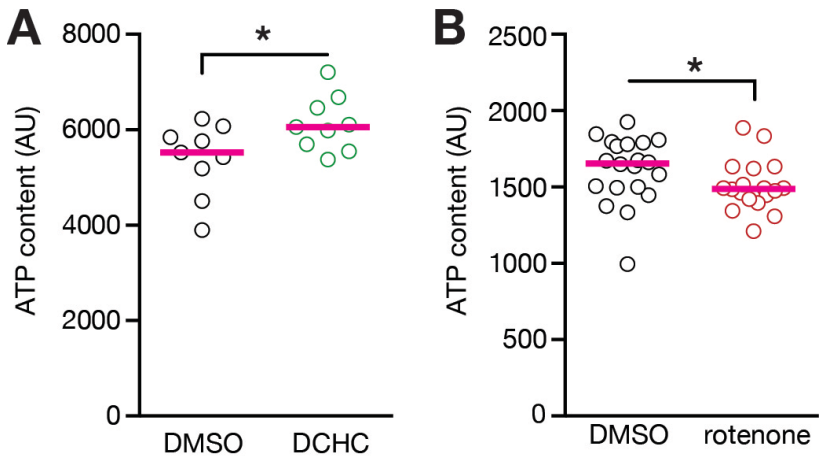

Figure S6: Pharmacological manipulation of mitochondria in human fibroblasts.

A, Treatment with DCHC significantly increases cellular ATP levels. Two-tailed student t test with Welch's correction, n=9/9, p=0.0334.

B, Treatment with rotenone reduces cellular ATP levels. Two-tailed Mann-Whitney test, n=20/18, p=0.0287.

The bar represents the median.

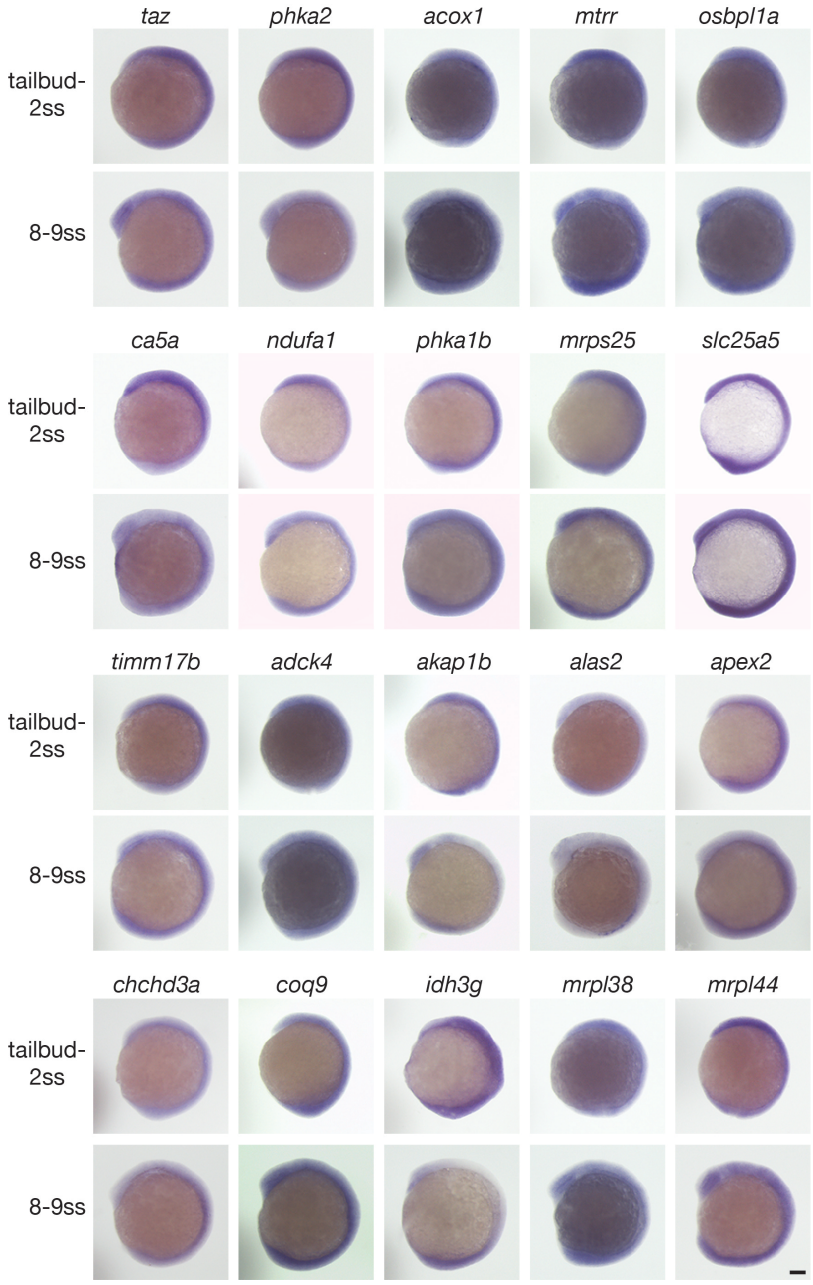

Figure S7: Mitochondria-associated genes identified as homozygous or hemizygous rare variants in heterotaxy patients are expressed in zebrafish embryos during developmental stages when symmetry breaking takes place. Shown are lateral views of embryos in tailbud/2 ss and 8-9 ss, respectively. Candidate gene is indicated on top, while stage is indicated on the left. Closest homologues to human genes were assessed in zebrafish. Scale bar: 100 µm.

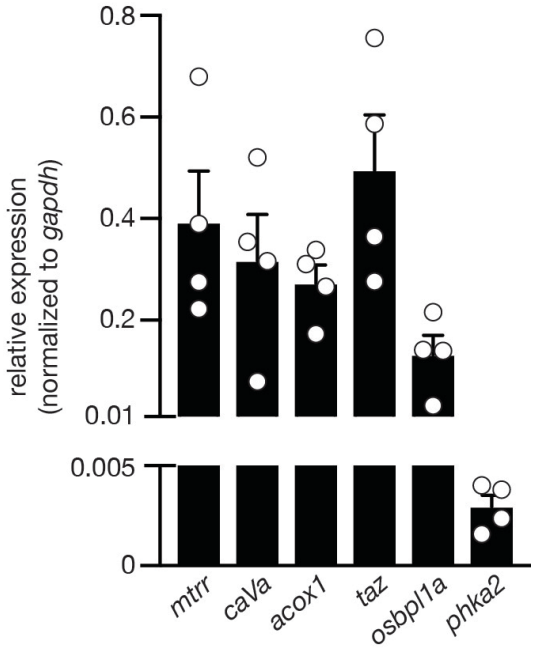

Figure S8: Expression levels of candidate genes in zebrafish embryos during developmental stage when KV cilia are functional (6-8 ss). Expression was qualitatively tested by qPCR and normalized to *gapdh* levels. n=4, mean ± SEM.

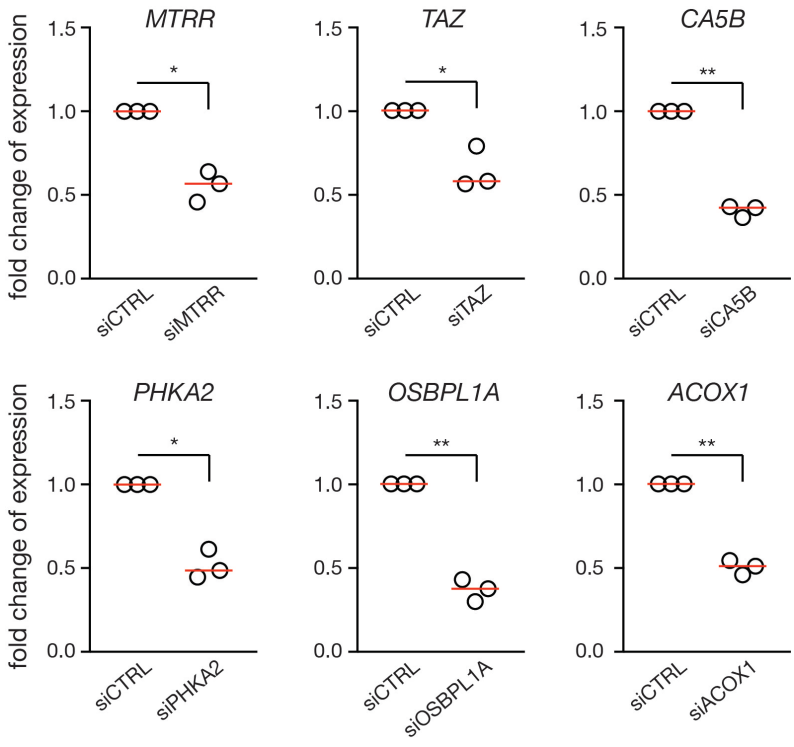

Figure S9: Verification of KD efficiency of candidate genes in human fibroblasts. Expression was analyzed by qPCR and first normalized to *SDHA* levels. Then expression was compared to control-transfected cells. Two-tailed, paired t-test, n=3, *MTRR* p=0.0138, *TAZ* p=0.0389, *CA5B* p=0.0012, *PHKA2* p=0.0106, *OSBPL1A* p=0.0036, *ACOX1* p=0.0025; the bar represents the median.

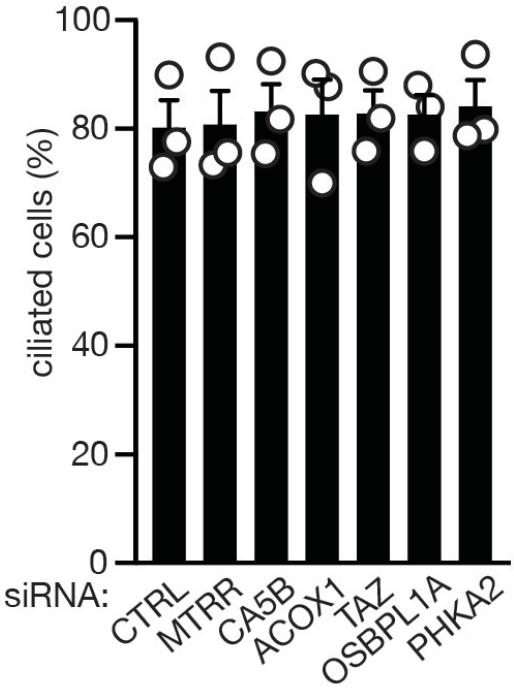

Figure S10: KD of candidate genes in human fibroblasts does not change the number of ciliated cells. One-way ANOVA with Holm-Sidak's correction, N=3, CTRL n=329, *MTRR* n=326, *TAZ* n=329, *CA5B* n=319, *PHKA2* n=329, *OSBPL1A* n=319, *ACOX1* n=318

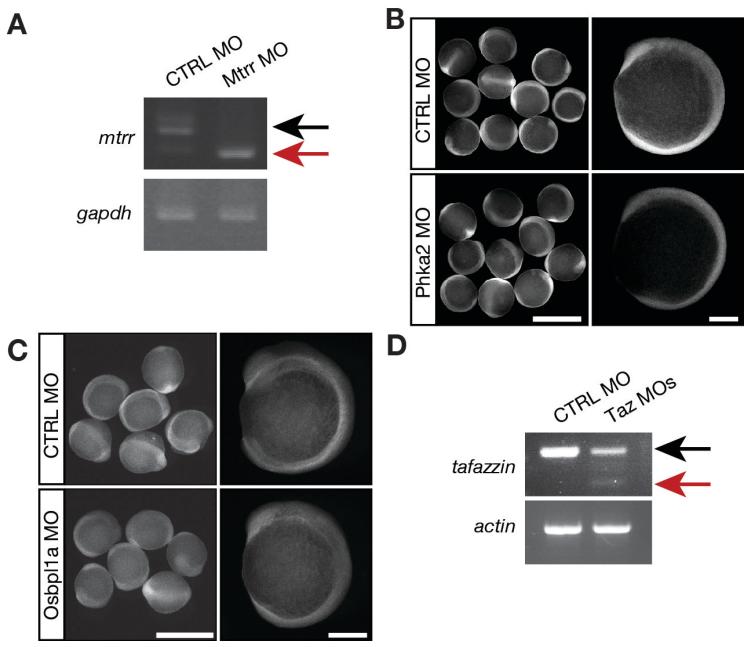

Figure S11: Verification of morpholino efficiency.

A, RT-PCR of control injected (CTRL MO) and splice blocking morpholino targeting Mtrr injected (Mtrr MO) embryos at 24 hpf. In embryos with Mtrr MO the original band at 393 bp partially disappeared. Instead a lower band could be detected. Sequencing revealed a 58 bp deletion, which includes the ATG of Mtrr. n=2 independent experiments.

B, Injection of zebrafish embryos with Phka2 splMO reduces expression of PHKA2 on protein level as determined by probing with an antibody specific for Phka2. Embryos shown at 6-8 ss stage. Scale bar in left panels 1 mm, in right panels 200 µm.

C, Injection of zebrafish embryos with Osbpl1a splMO reduces expression of Osbpl1a on protein level as determined by probing with an antibody specific for OSBPL1a at 8 ss. Scale bar in left panels 1 mm, in right panels 200 µm.

D, RT-PCR of control injected (CTRL MO) embryos and embryos simultaneously injected with a splice blocking MO targeting the 5'-end of exon 2 of zebrafish Taz and a previously published ATG MO (41) at 24 hpf. In embryos with Taz MOs the original band at 219 bp partially disappeared. Instead a lower band could be detected. Sequencing of this band confirmed aberrant splicing upon MO injection. n=3 independent experiments.

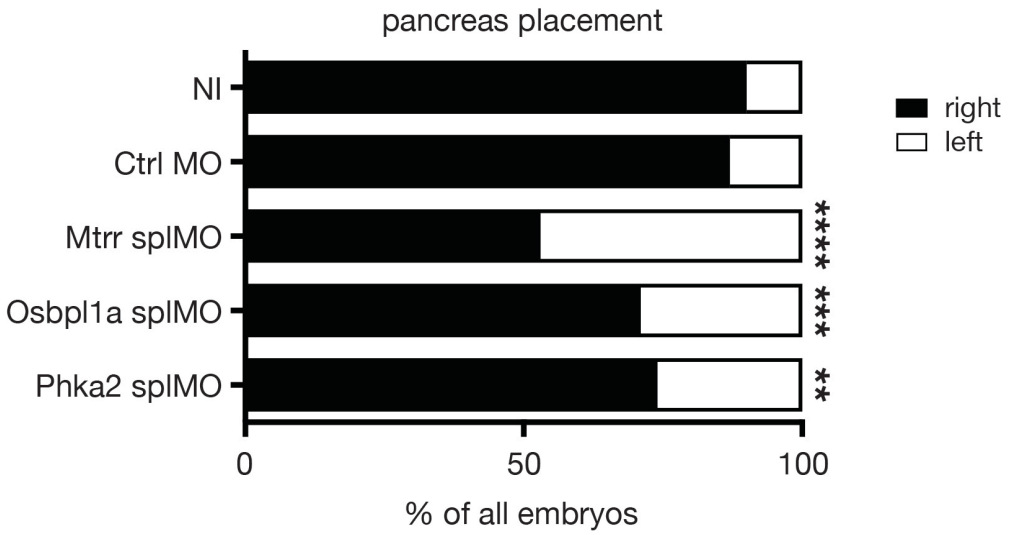

Figure S12: KD of candidate genes in developing zebrafish increases frequency of misplaced pancreas. N=9/9/3/6/4; n=231/203/49/143/104; Two-sided Fisher's exact test; all compared to Ctrl MO; Mtrr splMO $p<0.0001$; Osbpl1a splMO $p=0.0005$; Phka2 splMO $p=0.0072$.

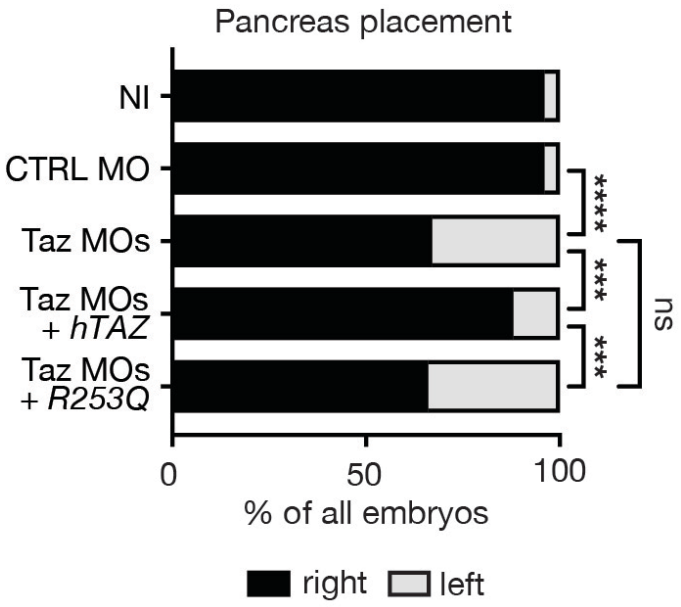

Figure S13: Only co-expression of wt*TAZ* RNA rescues aberrant pancreas placement after Taz KD. N=5; n=119/94/116/114/112; Two-sided Fisher's exact test; CTRL MO vs Taz MOs $p<0.0001$, Taz MOs vs Taz MOs +*hTAZ* $p=0.0002$, Taz MOs vs Taz MOs +R253Q $p=0.8888$, Taz MOs +*hTAZ* vs Taz MOs +R253Q $p=0.0001$.

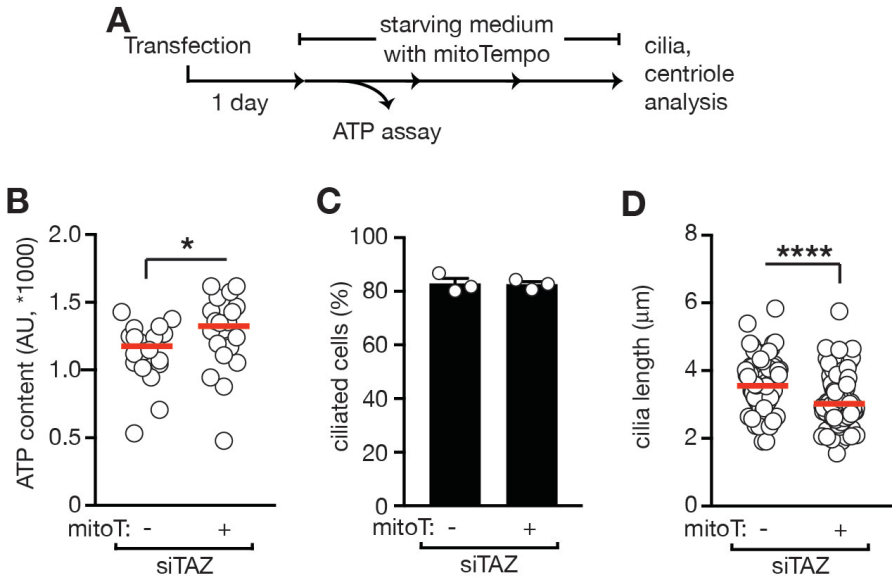

Figure S14: Number of ciliated fibroblast cells after KD of *TAZ* candidate gene and mitoTempo treatment.

A, Experimental outline of mitoTempo (mitoT, 50 nM) treatment.

B, MitoTempo treatment elevates ATP levels in *TAZ* KD cells. Two-tailed Mann-Whitney test, n=20/20, p=0.0436. The bar represents the median.

C, MitoTempo treatment does not impact the number of ciliated cells in *TAZ* KD cells. N=3, n=319/320. Shown is mean +/- SEM.

D, Shortening of cilia after mitoTempo treatment of *TAZ* KD cells. Two-tailed Mann-Whitney test, N=3, n=99/96, p<0.0001. The bar represents the median.

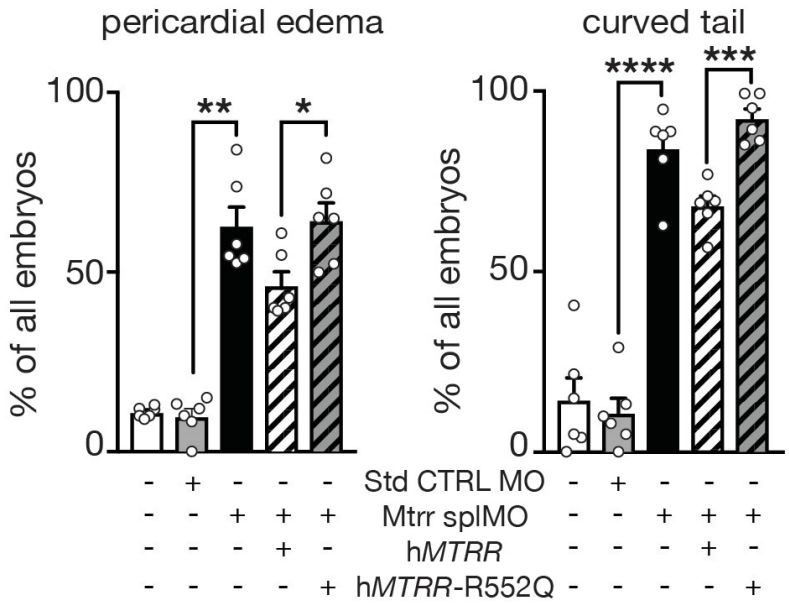

Figure S15: Co-injection of mRNA encoding the rare variant of the *MTRR* gene as detected in heterotaxy patient does not rescue ciliopathy-like phenotypes in Mtrr morphant zebrafish. Quantification of pericardial edema and curved tail after Mtrr KD. N=6, n=127/131/128/128/115; RM one-way ANOVA test with Holm-Sidak's multiple comparison; pericardial edema, CTRL MO vs Mtrr MO p=0.0021, Mtrr MOs vs Mtrr MOs+h*MTRR* p=0.0886, Mtrr MOs+h*MTRR* vs Mtrr MOs +R552Q p=0.0289;

Curved Tail, CTRL MO vs Mtrr MO p<0.0001, Mtrr MOs vs Mtrr MOs+h*MTRR* p=0.0592, Mtrr MOs+h*MTRR* vs Mtrr MOs +R552Q p=0.0006.

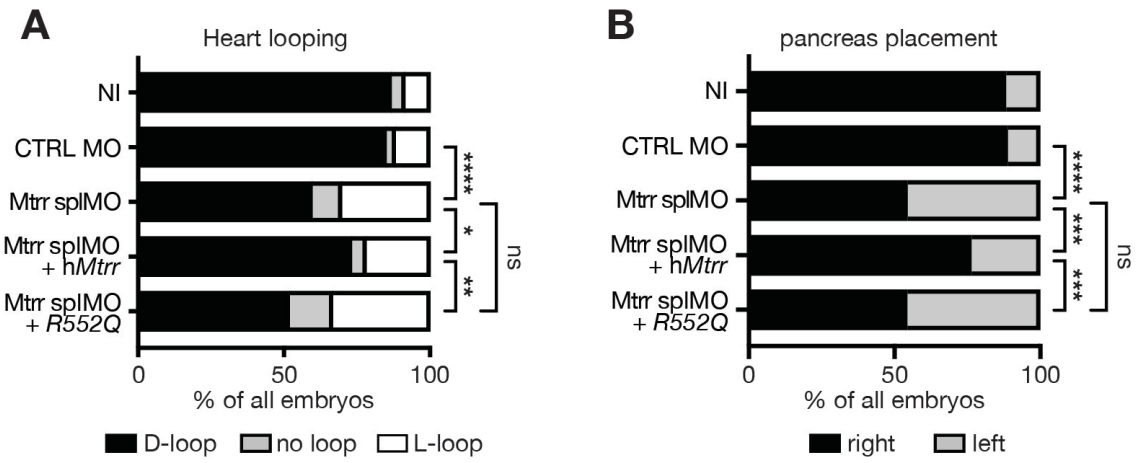

Figure S16: Overexpression of the rare variant MTRR-R552Q does not rescue aberrant L-R asymmetry induced by Mtrr KD.

A, Heart looping. N=5; n=128/126/119/119/114; Two-sided Fisher's exact test; CTRL MO vs Mtrr splMO p<0.0001, Mtrr splMO vs Mtrr splMO +h*MTRR* p=0.0392, Mtrr splMO vs Mtrr splMO +R552Q p=0.2375, Mtrr splMO + h*MTRR* vs Mtrr splMO +R552Q p=0.0011.

B, Pancreas position as assessed by *insulin in situ* hybridization. N=5; n=128/126/119/119/114; Two-sided Fisher's exact test; CTRL MO vs Mtrr splMO p<0.0001, Mtrr splMO vs Mtrr splMO +h*MTRR* p=0.0006, Mtrr splMO vs Mtrr splMO +R552Q p>0.9999, Mtrr splMO + h*MTRR* vs Mtrr splMO +R552Q p=0.0005.

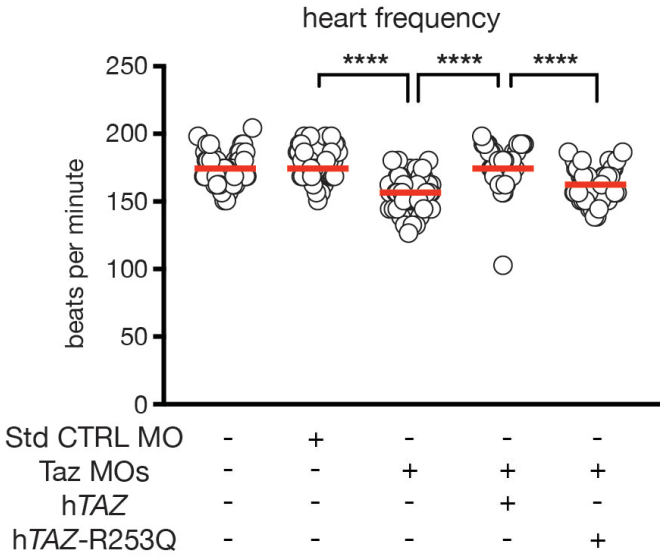

Figure S17: Patient variant (TAZ-R253Q) cannot rescue reduced heartbeat frequency caused by TAZ KD in zebrafish embryos. N=3, n=70/63/73/63/63, Kruskal-Wallis test with Dunn's multiple comparison; CTRL MO vs Taz MOs p<0.0001, Taz MOs vs Taz MOs +h*TAZ* p<0.0001, Taz MOs +h*TAZ* vs Taz MOs +R253Q p<0.0001.

The bar represents the median.

Table S1: Description of heart defects and age at time point of sample collection of patients with CHD not known to be related to dysfunctional cilia. CHDs are abbreviated as follows: atrial septal defect (ASD), coarctation of the aorta (CoA), transposition of the great arteries with intact ventricular septum (TGA (IVS)), tetralogy of fallot (TOF), ventricular septal defect (VSD).

Sample #	sex	Heart defect	Age at time of surgery
1	female	ASD	44 y
2	male	ASD	15 y
3	female	ASD	69 y
4	female	CoA	42 y
5	male	CoA	15 y
6	male	CoA	19 y
7	male	TGA (IVS)	11 y
8	male	TGA (IVS)	28 y
9	male	TOF	41 y
10	male	TOF	16 y
11	female	TOF	13 y
12	male	TOF	49 y
13	female	VSD	3 y
14	female	VSD	7 y
15	female	VSD	28 y
16	female	VSD	20 y
17	female	VSD	1 m
18	male	VSD	40 y
19	female	VSD	9 y
20	female	VSD	28 y

Table S2: Mitochondria-associated genes assessed in American heterotaxy cohort

Table provided as separate Excel file.

Table S3: Allele frequency of identified variants in different ethnic backgrounds according to ExAC server.

Gene Names	allele frequency (homozygous or hemizygous)							
	all	Latino	African	East Asian	European (Finnish)	European (Non-Finnish)	Other	South Asian
ACOX1	6.589E-05	0	3.84E-04	0	0	3.00E-05	0	1.21E-04
ACSM2A	1.647E-05	0	0	0	0	3.00E-05	0	0
ADCK4	1.553E-03	3.47E-04	0	0	3.33E-03	2.37E-03	2.21E-03	0.000121256
AKAP1	4.340E-04	1.87E-04	0	0	0	7.47E-04	0	1.39E-04
CHCHD3	0	0	0	0	0	0	0	0
COQ9	1.010E-04	1.78E-04	0	0	0	3.05E-05	0	4.96E-04
MRPL38	0	0	0	0	0	0	0	0
MRPL44	0	0	0	0	0	0	0	0
MRPS25	0	0	0	0	0	0	0	0
MTRR	na	na	na	na	na	na	na	na
OSBPL1A	3.295E-05	0	0	0	0	5.99E-05	0	0
ALAS2	8.524E-05	0	0	0	0	1.25E-04	0	1.46E-04
ALAS2	6.505E-04	0	1.19E-04	0	2.29E-04	9.49E-04	0	9.51E-04
APEX2	1.134E-03	3.24E-04	0	1.52E-04	1.55E-03	1.75E-03	0	1.58E-04
APEX2	1.168E-05	0	0	0	0	2.13E-05	0	0
CA5B	na	na	na	na	na	na	na	na
IDH3G	na	na	na	na	na	na	na	na
NDUFA1	2.372E-03	0	2.35E-04	0	2.65E-03	3.73E-03	1.58E-03	1.38E-03
PHKA1	na	na	na	na	na	na	na	na
PHKA2	8.999E-05	0	0	0	0	1.71E-04	0	0
SLC25A5	na	na	na	na	na	na	na	na
SLC25A53	na	na	na	na	na	na	na	na
*SLC25A53**	na	na	na	na	na	na	na	na
*SLC25A53**	na	na	na	na	na	na	na	na
TAZ	0	0	0	0	0	0	0	0
TIMM17B	na	na	na	na	na	na	na	na

Table S4: List of control genes extracted from the 1000 Genomes to perform statistical analysis of the abundance of rare mitochondria-associated gene variants in heterotaxy patients

Four sets of genes were chosen: Genes associated with autism, cancer or two sets of randomly picked unrelated disease genes. Table provided as separate Excel file.